Terra Nova

Direct 40Ar/39Ar K-feldspar dating of Late Permian - Early Triassic brittle faulting in northern Norway

Journal:	*Terra Nova*
Manuscript ID	TER-2017-0117.R1
Wiley - Manuscript type:	Paper
Date Submitted by the Author:	n/a
Complete List of Authors:	Davids, Corine; Norut Northern Research Institute; University of Tromsø, Department of Geology Benowitz, Jeffrey; University of Alaska Fairbanks, Geophysical Institute Layer, Paul; University of Alaska Fairbanks, Geophysical Institute Bergh, Steffen; University of Tromsø, Department of Geology
Keywords:	Brittle Faulting, 40Ar/39Ar K-Feldspar geochronology, Post-Caledonian, Northern Norway, Late Permian - Early Triassic

Direct $^{40}Ar/^{39}Ar$ K-feldspar dating of Late Permian - Early Triassic brittle faulting in northern Norway

Corine Davids[1,2], Jeff A. Benowitz[3*], Paul W. Layer[4], Steffen G. Bergh[2]

[1]Norut Northern Research Institute, NO-9294 Tromsø, Norway

[2]Department of Geosciences, UiT The Arctic University of Norway, NO-9037 Tromsø, Norway

[3]Corresponding author: Geophysical Institute, University of Alaska Fairbanks, Fairbanks, AK 99775-5940, USA, jbenowitz@alaska.edu, 907-474-7010*

[4]College of Natural Science and Mathematics, University of Alaska Fairbanks, Fairbanks, AK 99775-5940, USA

ABSTRACT

While the offshore post Caledonian extensional history of the north Norwegian passive margin is well constrained, the tectonic relationship between onshore and offshore regions is less clear because of limited age constraints on the timing of rifting onshore. $^{40}Ar/^{39}Ar$ dating of K-feldspar from hydrothermally altered fault rocks in a Precambrian gneiss complex in northern Norway was used to study the timing of extensional faulting onshore. In addition, $^{40}Ar/^{39}Ar$ dating of K-feldspar from the host rock provided insight into the regional rock cooling history prior to brittle deformation. Results indicated a dominant Late Permian – Early Triassic (~265-244 Ma) faulting event and found no evidence for later reactivation, which has been documented offshore. The region cooled to below the closure temperature for $^{40}Ar/^{39}Ar$ K-feldspar in the Carboniferous to Early Permian, prior to the main brittle faulting event. $^{40}Ar/^{39}Ar$ dating of fault zone.

1. INTRODUCTION

The Norwegian passive margin was formed during a ~300 My period of extension and rifting that followed Caledonian orogenesis. The extensional history of the continental shelf of northern Norway and the Barents Sea is well understood through the study of seismic and well data (e.g. Tsikalas et al., 2012; Hansen et al., 2012; Clark et al., 2013; Indrevær et al. 2013, 2014; Koehl et al. 2017), but less is known about the onshore post-Caledonian history. Constraining the timing of the brittle fault activity and exhumation in the coastal areas of northern Norway is therefore essential for understanding the relationship between offshore and onshore tectonics and the implications for the extensional tectonic history of the North Atlantic margin.

Brittle faults in crystalline terrains are often difficult to date. The fault cores, which may contain dateable clay minerals in fault gouge or fault breccia, are often not exposed, and the lack of sedimentary strata precludes relative age determination. Outcrops with fault gouge are rare in western Troms, northern Norway, but three faults were determined as Permian through K-Ar illite geochronology (Davids et al., 2013) and paleomagnetic dating (Olesen et al., 1997). However, several fault and fracture zones are associated with hydrothermal alteration which, in granitic rocks, is visible as a red discoloration within fault zones and around fractures. The infiltration of hot fluids associated with faulting can potentially fully reset the $^{40}Ar/^{39}Ar$ isotopic system in K-feldspar, in which case the apparent age can be interpreted to be close in time to the faulting event (e.g. Steltenpohl et al., 2011).

This paper compares new K-feldspar $^{40}Ar/^{39}Ar$ ages from brittle fault and fracture zones with results from host rock K-feldspar, and demonstrates that the hydrothermally altered K-feldspar were indeed fully reset during fracturing and associated hot fluid infiltration. These results are used to estimate the timing of brittle faulting onshore in northern Norway and combined with the regional cooling history obtained from host rock K-feldspar to correlate the identified onshore post-Caledonian tectonic history with tectonic events offshore along the north Atlantic margin and in the SW Barents Sea.

2. REGIONAL GEOLOGY

The study area (Figs. 1 and 2) is located on the North Atlantic passive margin across the transition from the rifted Lofoten-Vesterålen margin to the sheared SW Barents Sea margin (Faleide et al., 1993, 2008; Tsikalas et al., 2012). The North Atlantic passive margin started to develop following Caledonian orogenic collapse in the Late Devonian to Carboniferous. Rifting took place during a succession of pronounced rift phases from the Carboniferous to the

Paleogene (e.g. Ziegler, 1989; Lundin and Doré, 1997; Mosar et al., 2002; Clark et al., 2013) and resulted in continental break-up and drifting in the Paleogene (e.g. Talwani and Eldholm, 1977; Olesen et al., 2007).

Paleozoic extension and rifting is thought to have been influenced by the structural framework inherited from the Caledonian orogeny in the Ordovician to Early Devonian (Gudlaugsson et al., 1998; Clark et al., 2013; Gernigon et al., 2014). The SW Barents Sea was the tectonic intersection between the NE-trending Scandinavian Caledonides, the N-trending Svalbard Caledonides to the north and the NW-trending Timanides to the east (Gudlaugsson et al., 1998; Gee and Pease, 2004). Post Caledonian brittle fault zones on the Lofoten-Vesterålen margin are dominated by NNE-SSW and ENE-WSW trends (Figs. 1 and 2); in contrast, basins and ridges in the SW Barents Sea form a fan-shaped structure (Fig. 1), with N-S trending fault zones in the west linking up with the Arctic rift (Gudlaugsson et al., 1998).

The geology of the study area (Fig. 2) is comprised of a Precambrian gneiss complex, the West Troms Basement Complex (WTBC) (Bergh et al., 2010), which forms a NE-SW trending basement horst extending northward on the Finnmark Platform offshore (Koehl et al. 2017). The WTBC is separated from a stack of Caledonian nappes to the east by Caledonian thrusts and post-Caledonian brittle normal faults (Andresen and Forslund, 1987; Olesen et al., 1997; Indrevær et al. 2014), and from a series of deep offshore basins filled with Late Paleozoic to Quaternary sedimentary rocks to the west (Gabrielsen et al., 1990; Hansen et al., 2012; Gudlaugsson et al., 1998; Tsikalas et al., 2012; Indrevær, et al., 2013; Faleide et al., 2017).

Unlike similar Precambrian gneiss complexes in southern Norway, which experienced high pressure metamorphism during the Scandian phase of Caledonian orogeny (e.g. Roberts, 2003), the WTBC was only weakly influenced by Caledonian deformation, and Precambrian tectono-metamorphic structures are well preserved (Corfu et al., 2003; Bergh et al., 2010). The presence of Proterozoic $^{40}Ar/^{39}Ar$ hornblende ages throughout the WTBC indicate that the WTBC has not experienced temperatures over ~500°C during the Caledonian orogeny (Dallmeyer, 1992). WTBC brittle faulting occurred in the Permian (Olesen et al., 1997; Davids et al., 2013) and was regionally followed by cooling from ~120˚C-60˚C in the Late Permian – Early Triassic based on apatite fission track analysis (Davids et al., 2013).

3. SAMPLE DESCRIPTIONS

Eleven K-feldspar samples were analyzed: six from undeformed granite host rock and five samples from brittle fault zones. The host rock samples were collected from across the WTBC in order to reconstruct the regional cooling history. In contrast, the brittle fault samples come from the southwestern part of the WTBC, where the intensity and frequency of brittle deformation is higher than in the northeast.

Host rock samples were collected from macroscopically undeformed granite or granitic dykes. K-feldspar in host rock samples show some low temperature deformation with minor recrystallization along grain boundaries and undulose extinction, but to a lesser extent than the fault samples. The sampled brittle fault zones are all located in weakly deformed Proterozoic granite and are oriented either NNE-SSW (samples S08/46, S10/32 and S09/20) or ENE-WSW (samples S11/6 and S11/21), the same two orientations that are dominant offshore. The fault zones are generally steeply dipping (> 60˚), but their orientation is locally influenced by an existing gneissic foliation (e.g. Tussøya S10/32). Lineations, if present, are mostly steep. The fault zones are characterized by 5-50 m wide zones of strongly fractured red-colored granite with abundant chlorite and hematite-coated fracture surfaces. Epidote veins and (ultra)cataclasite occur in the cores of some of the zones; fault gouge was found in the fault zone in Sifjord (Senja), 5 km along strike of the sample location S11/21 (Fig. 2). Illite separated from this fault gouge yielded a K-Ar maximum age of ~293 Ma (Davids et al., 2013). The fault samples were collected from the red-colored granite associated with the brittle fault zones. K-feldspar in all brittle samples display extensive sub grain formation along grain boundaries, undulose extinction and microfracturing (Fig. 3), indicating temperatures < ~400˚C (Passchier and Trouw, 2005). K-feldspar is mostly clear microcline, but some grains contain domains of perthite.

4. $^{40}Ar/^{39}Ar$ RESULTS

Descriptions of the sample locations, analytical procedures, data tables, and age spectra can be found in DR1, DR2 and DR3. Host rock samples gave complex spectra. Four samples from the southern two islands (Kvaløya and Senja, Fig. 2) show apparent ages of ~280-300 Ma in the initial 20-30% of the spectra which subsequently increase to ~350-500 Ma (Fig. 4B and Table 1). Two samples from the northern two islands (Vanna and Ringvassøya, Fig. 2) yield apparent ages of ~350-370 Ma in the initial ca 40% of the gas release followed by an increase to over 400 Ma (Fig. 4C and Table 1). Intermediate age maxima in samples EG and R3 indicate the presence of excess Ar, based on the correlation between individual analysis old apparent ages and high Cl/K ratios and the known link between Cl/K ratios and melt inclusions in K-feldspar (Harrison et al., 1994). In contrast, all 5 brittle samples show similar flat age spectra with the majority of the apparent plateau and weighted average ages between ~ 240-280 Ma (Fig. 4A and Table 1); integrated ages (excluding outliers with evidence of excess ^{40}Ar) vary between ~267-245 Ma.

5. REGIONAL COOLING

In the Caledonian nappes immediately east of the WTBC, $^{40}Ar/^{39}Ar$ hornblende and muscovite ages of ~ 430-425 Ma and ~425-400 Ma recorded cooling following peak metamorphism (Coker et al., 1995; Dallmeyer and Andresen, 1992) during the main phase of nappe emplacement, the Scandian event at ~430-400 Ma (e.g. Roberts, 2003). In the WTBC, however, the presence of Proterozoic $^{40}Ar/^{39}Ar$ hornblende ages (Dallmeyer, 1992) and pre-Caledonian $^{40}Ar/^{39}Ar$ muscovite ages (Davids et al., 2012) throughout the WTBC confirmed field observations that the WTBC is only weakly affected by Caledonian deformation and metamorphism (Dallmeyer, 1992; Corfu et al., 2003; Bergh et al., 2010). Although three of the host rock samples show signs of excess Ar (intermediate age maxima, EG and R3, or increasing Cl/K ratios in the higher temperature steps, S10/40), three other host rock samples record apparent ages of ≥350 Ma in the higher temperature steps without indication of excess Ar. These new results suggest that the regional temperature in the WTBC was below ~400˚C by the end of the Caledonian orogeny.

The region cooled to below the K-feldspar closure temperature by ~280 Ma as shown by the apparent ages of ~280-370 Ma in the low temperature steps. The difference in initial ages of ~280-320 Ma for host rock K-feldspar in the southwest and ~350-370 Ma in the northeast is intriguing. It implies either that the host rock K-feldspar in the southwestern part are affected to some extent by regional Permian fault events (Eide et al., 1997), or that the northeastern part cooled earlier than the southwestern part. The latter would imply either a vertical offset, possibly due to Permian faulting, or tilting with the northeastern part subsiding relative to the southwestern part of the WTBC.

6. TIMING OF BRITTLE DEFORMATION

The flat $^{40}Ar/^{39}Ar$ age spectra from the fault samples (Fig. 4A) indicate that these samples experienced resetting due to a thermal disturbance at ~250 Ma. The lack of a step-wise increase in apparent ages in the low temperature steps of the age spectra suggests that this thermal event took place while the regional temperature was already below the Ar closure temperature for K-feldspar at ~200˚C. The latter is supported by the age spectra of the host rock samples from the southwestern part of the WTBC, which show initial apparent ages between ~300 and ~280 Ma (EG, S09/18 and S11/20) (Fig. 4B). The K-feldspar grains in the fault zone samples show varying amounts of recrystallization and microfracturing (Fig. 3). The precipitation of epidote and hematite on fracture surfaces, which locally display slickenslides, and the red coloration of granitic rocks indicate the infiltration of fluid simultaneous with brittle deformation. It is, therefore, likely that a combination of brittle deformation and associated fluid infiltration caused the resetting of the Ar isotopic system in the brittle K-feldspar between ~265 and ~244 Ma. This is ~20-40 My younger than previous estimates of the timing of brittle faulting in the WTBC, but similar to brittle faults identified further south in Norway (e.g. Eide et al., 1997). K-Ar dating of 2 fault gouges from major faults in the WTBC gave maximum ages of ~ 293-284 Ma for the formation of illite in the fault gouge (Davids et al., 2013), while paleomagnetic dating of brittle fault rocks in the WTBC has previously demonstrated two periods of brittle faulting, an early Permian phase overprinted by a Paleogene-recent phase (Olesen et al., 1997). The initial apparent ages of the host rock samples, ~300-280 Ma (Fig. 4B), correspond well with these published ages from fault gouges and paleomagnetic dating. The younger $^{40}Ar/^{39}Ar$ ages for the brittle K-feldspar samples could be explained by two different scenarios: ***1.*** The brittle K-feldspar ages can be interpreted to indicate a second phase of faulting associated with hot fluid infiltration. ***2.*** Alternatively, the microfracturing and grain size reduction (Fig. 3), induced by brittle faulting and hot fluid infiltration, reduced the diffusion length sufficiently to result in further Ar loss in the fault samples after the faulting event compared to the host rock samples. In the latter case, one would expect to see a diffusion profile with increasing apparent ages in the low temperature steps of the age spectra. However, as the age spectra are flat, we prefer to interpret the data to be the result of two separate periods of fault activity: early localized faulting in the Early Permian (~300-280 My), resulting in a small number of major faults as documented regionally (Eide et al., 1997; Blaich et al., 2017), followed by more widespread fracturing and reactivation, particularly in the southwestern part of the WTBC, associated with hot fluid infiltration in the Late Permian-Triassic (~265-244 My).

7. TECTONIC IMPLICATIONS

The dated faulting in the WTBC was part of a widespread Late Permian – Early Triassic rifting event, which has been recognized throughout the North Atlantic and Arctic regions. In the SW Barents Sea, rifting started in the Early-Mid Carboniferous (Koehl et al. 2017) and was followed by Mid to Late Triassic post-rift thermal subsidence and an influx of coastal and alluvial sediments that were probably derived from the Fennoscandian Shield (e.g. Clark et al., 2013; Gudlaugsson et al., 1998; Smelror et al., 2009; Torgersen et al., 2014). At the same time, Late Permian – Early Triassic fault activity in the WTBC was followed by cooling to ~60˚C in the Early to Mid Triassic (Davids et al., 2013). Since faulting and associated hot fluid infiltration took place when the temperature in the WTBC block was below the K-feldspar closure temperature, we can estimate that faulting was associated with ~4-5 km of uplift and subsequent exhumation to a depth of ~2-3 km (assuming a regional geotherm of ~25-30˚C/km; e.g. Hendriks, 2003). The same Early to Mid Triassic cooling was also reported from the region east of the WTBC, indicating that the whole area exhumed at the same time without significant offset along the VVFC (Fig. 1) that forms the eastern boundary of the WTBC. This suggests that the main movement may have taken place along the western boundary of the WTBC, the TFFC (Fig. 1). The ~4-5 km of erosion that must have taken place in these onshore areas is likely to have contributed to the thick Triassic deposits in the Barents Sea. There is to date no indication that subsequent rifting events in the Jurassic-Cenozoic, which have been recognized both offshore and in the Vesterålen-Lofoten region to the southwest, have significantly affected the WTBC.

8. CONCLUSION

Fluid infiltration is often associated with normal faulting (Sibson, 2000). This study demonstrates the usefulness of applying $^{40}Ar/^{39}Ar$ analysis to K-feldspar from brittle fault and fracture zones to better constrain the history of brittle faulting and fluid infiltration. Combined with the regional cooling history obtained from the host rock, the results presented here indicate that the WTBC cooled to below ~200˚C prior to a dominant faulting event in the Late Permian – Early Triassic (~265-244 My). This event is associated with a major rifting event in the SW Barents Sea and along the North Atlantic margin. No evidence has been found for later reactivation.

ACKNOWLEDGEMENTS

The work was carried out as part of the larger Onshore-Offshore project led by Steffen Bergh. We thank Det Norske and Statoil for financial support. We thank Victoria Pease, an anonymous reviewer and, editors Klaus Mezger and Klaudia Kuiper for constructive and helpful reviews and suggestions that improved the manuscript.

REFERENCES CITED

Andresen, A. and Forslund, T., 1987. Post-Caledonian Brittle Faults in Troms: Geometry, Age and Tectonic Significance. *The Caledonian and Related Geology of Scandinavia conference*, Cardiff, 22–23 September.

Bergh, S.G., Kullerud, K., Armitage, P.E.B., Zwaan, K.B., Corfu, F., Ravna, E.J.K. and Myhre, P.I. 2010. Neoarchaean to Svecofennian tectono-magmatic evolution of the West Troms Basement Complex, North Norway. *Norwegian Journal of Geology*, **90**, 21–48.

Blaich, O.A., Tsikalas, F. and Faleide, J.I., 2017. New insights into the tectono-stratigraphic evolution of the southern Stappen High and its transition to Bjørnøya Basin, SW Barents Sea. *Marine and Petroleum Geology*, **85**, 89-105, doi: 10.1016/j.marpetgeo.2017.04.015.

Clark, S.A., Glorstad-Clark, E., Faleide, J.I., Schmid, D., Hartz, E.H. and Fjeldskaar, W., 2013. Southwest Barents Sea rift basin evolution: comparing results from backstripping and time-forward modeling. *Basin Research*, **25**, 1–17, doi: 10.1111/bre.12039.

Coker, J.E., Steltenpohl, M.G., Andresen, A. and Kunk, M.J., 1995. An 40Ar/39Ar thermochronology of the Ofoten-Troms region: implications for terrane amalgamation and extensional collapse of the northern Scandinavian Caledonides. *Tectonics*, **14**, 435–447.

Corfu, F., Armitage, P.E.B., Kullerud, K. and Bergh, S.G., 2003. Preliminary U–Pb geochronology in the West Troms Basement Complex, North Norway: Archaean and Palaeoproterozoic events and younger overprints. *Norges Geologiske Undersøkelse Bulletin*, **441**, 61–72.

Dallmeyer, R.D., 1992. ^{40}Ar/^{39}Ar mineral ages within the Western Gneiss Terrane, Troms, Norway: evidence for polyphase Proterozoic tectonothermal activity (Svecokarilian and Sveconorwegian). *Precambrian Research*, **57**, 195–206.

Dallmeyer, R.D. and Andresen, A., 1992. Polyphase tectonothermal evolution of exotic Caledonian nappes in Troms, Norway: evidence from 40Ar/39Ar mineral ages. *Lithos*, **29**, 19–42.

Davids, C., Benowitz, J.A. and Layer, P., 2012. Constraining the Caledonian Tectonic Overprint in a Precambrian Gneiss Terrane in Northern Norway. *International Conference on Thermochronology*, 13th, Guilin, China, Abstracts.

Davids, C., Wemmer, K., Zwingmann, H., Kohlmann, F., Jacobs, J. and Bergh, S.G., 2013. K–Ar illite and apatite fission track constraints on brittle faulting and the evolution of the northern Norwegian passive margin. *Tectonophysics*, **608**, 196–211, doi: 10.1016/j.tecto.2013.09.035.

Eide, E.A., Torsvik, T.H. and Andersen, T.B., 1997. Absolute dating of brittle fault movements: Late Permian and Late Jurassic extensional fault breccias in western Norway. *Terra Nova*, **9**, 135–139.

Faleide, J.I., Vågnes, E. and Gudlaugsson, S.T., 1993. Late Mesozoic–Cenozoic evolution of the south-western Barents Sea in a regional rift-shear tectonic setting. *Marine and Petroleum Geology*, **10**, 186–214.

Faleide, J.I., Tsikalas, T., Breivik, A.J., Mjelde, R., Ritzmann, O., Engen, Ø., Wilson, J. and Eldholm, O., 2008. Structure and evolution of the continental margin off Norway and the Barents Sea. *Episodes*, **31**, 82–91.

Faleide, J.I., Pease, V., Curtis, M., Klitzke, P., Minakov, A., Scheck-Wenderoth, M., Kostyuchenko, S. and Zayonchek, A., 2017. Tectonic implications of the lithospheric structure across the Barents and Kara shelves. In: *Circum Arctic Lithosphere Evolution* (V.

Pease and B. Coakley, eds), *Geological Society of London Special Publication*, **460**, 285-314, doi: 10.1144/SP460.18.

Gabrielsen, R.H., Færseth, R.B., Jensen, L.N., Kalheim, J.E. and Riis, F., 1990. Structural elements of the Norwegian continental shelf — part I: the Barents Sea Region. *Norwegian Petroleum Directorate Bulletin*, **6**, 1–33.

Gernigon, L., Brönner, M., Roberts, D., Olesen, O., Nasuti, A. and Yamasaki, T., 2014. Crustal and basin evolution of the southwestern Barents Sea: from Caledonian orogeny to continental breakup. *Tectonics*, doi: 10.1002/2013TC003439.

Gudlausson, S.T., Faleide, J.I., Johansen, S.E. and Breivik, A.J., 1998. Late Palaeozoic structural development of the South-western Barents Sea. *Marine and Petroleum Geology*, **15**, 73–102.

Hansen, J.-A., Bergh, S.G. and Henningsen, T., 2012. Mesozoic rifting and basin evolution on the Lofoten and Vesterålen Margin, North-Norway; time constraints and regional implications. *Norwegian Journal of Geology*, **91**, 203–228.

Harrison, T.M., Heizler, M.T., Lovera, O.M., Wenji, C. and Grove, M., 1994. A chlorine disinfectant for excess argon released from K-felsspar during step heating. *Earth and Planetary Science Letters,* **123**, 95-104.

Indrevær, K., Bergh, S.G., Koehl, J.-B., Hansen, J.-A., Schermer, E.R. and Ingebrigtsen, A., 2013. Post-Caledonian brittle fault zones on the hyper- extended SW Barents Sea Margin: New insights into onshore and offshore margin architecture. *Norwegian Journal of Geology,* **93**, 167–188.

Indrevær, K, Stunitz, H. and Bergh, S.G., 2014. On Palaeozoic-Mesozoic brittle normal faults along the SW Barents Sea margin: fault processes and implications for basement permeability and margin evolution. *Journal of the Geological Society*, London. **171**, 831-846, doi: 10.1144/jgs2014-018.

Koehl, J-B., Bergh, S.G., Henningsen, T., and Faleide, J-I. 2017. Mid/Late Devonian-Carboniferous collapse basins on the Finnmark Platform and in the southwesternmost Nordkapp basin, SW Barents Sea. *Solid Earth Discuss.*, doi:10.5194/se-2017-124.

Lundin, E.R. and Doré, A.G., 1997. A tectonic model for the Norwegian passive margin with implications for the NE Atlantic; Early Cretaceous to break-up. *Journal of the Geological Society*, London, **154**, 545–550.

Mosar, J., Eide, E.A., Osmundsen, P.T., Sommaruga, A. and Torsvik, T.H., 2002,.Greenland — Norway separation: a geodynamic model for the North Atlantic. *Norwegian Journal of Geology*, **82**, 281–298.

Olesen, O., Torsvik, T.H., Tveten, E., Zwaan, K.B., Løseth, H. and Henningsen, T., 1997. Basement structure of the continental margin in the Lofoten–Lopphavet area, northern Norway: constraints from potential field data, on-land structural mapping and palaeomagnetic data. *Norsk Geologisk Tidsskrift*, **77**, 15–30.

Olesen, O., Ebbing, J., Lundin, E., Mauring, E., Skilbrei, J.R., Torsvik, T.H., Hansen, E.K., Henningsen, T., Midbøe, P. and Sand, M., 2007. An improved tectonic model for the Eocene opening of the Norwegian-Greenland Sea: use of modern magnetic data. *Marine and Petroleum Geology*, **24**, 53–66.

Osmundsen, P.T., Sommaruga, A., Skilbrei, J.R. and Olesen, O., 2002. Deep structure of the Mid Norway rifted margin. *Norwegian Journal of Geology*, **82**, 205–224.

Passchier, C.W. and Trouw, R.A.J., 2005. *Microtectonics*. Springer, 366 pp.

Roberts, D., 2003. The Scandinavian Caledonides: event chronology, palaeogeographic settings and likely modern analogues. *Tectonophysics*, **365**, 283–299.

Sibson, R.H., 2000. Fluid involvement in normal faulting. *Journal of Geodynamics*, **29(3-5),** 469-499.

Smelror, M., Petrov, O., Larssen, G.B. and Werner, S., editors, 2009. *Atlas: Geological History of the Barents Sea*. Trondheim, Geological Survey of Norway, 135 pp.

Steltenpohl, M.G., Moecher, D., Andresen, A., Ball, J., Mager, S. and Hames, W.E., 2011. The Eidsfjord shear zone, Lofoten-Vesterålen, north Norway: an Early Devonian, paleoseismogenic low-angle normal fault. *Journal of Structural Geology*, **33**, 1023-1043.

Talwani, M. and Eldholm, O., 1977. Evolution of the Norwegian-Greenland Sea. *Geological Society of America Bulletin*, 88, 969–999.

Torgersen, E., Viola, G., Zwingmann, H. and Harris, C. 2014. Structural and temporal evolution of a reactivated brittle-ductile fault – Part II: Timing of fault initiation and reactivation by K-Ar dating of synkinematic illite/muscovite. *Earth and Planetary Science Letters*, **407**, 221-233.

Tsikalas, F., Faleide, J.I., Eldholm, O. and Blaich, O.A., 2012. The NE Atlantic conjugate margins. In: *Phanerozoic Passive Margins, Cratonic Basins and Global Tectonic Maps* (D. Roberts and A.W. Bally, eds.) Elsevier, 141–201.

Ziegler, P.A., 1989. Evolution of the North Atlantic; an overview. *American Association of Petroleum Geologists Memoir*, **46**, 111–129.

FIGURE CAPTIONS

Table 1. $^{40}Ar/^{39}Ar$ K-feldspar (KS) step heating results.

Figure 1. Geological overview map of the North Norwegian margin. Simplified after Mosar et al., (2002) and Faleide et al., (2008). BB: Bjørnøya Basin; FP: Finmark Platform; HB: Harstad Basin; HfB: Hammerfest Basin; LH: Loppa High; LR: Lofoten Ridge; RH: Røst High; SB: Sørvestsnaget Basin; TB: Tromsø Basin; TKF: Trollfjord-Komagelv Fault; TP: Trøndelag Platform; TFFC: Troms-Finmark Fault Complex; VB: Vøring Basin; VfB: Vestfjorden Basin; VVFC: Vestfjorden-Vanna Fault Complex.

Figure 2. Simplified map of the sample area with sample locations. Fs: K-feldspar; SEF: Stongelandseidet Fault; TFFC: Troms-Finmark Fault Complex; VF: Vannareid Fault; VVFC: Vestfjorden-Vanna Fault Complex. K: Kvaløya; S: Senja; R: Ringvassøya; V: Vanna.

Figure 3. Representative photomicrographs of K-feldspar (KS) from hydrothermally altered fault rocks. A. Microfractures in S08/46A. B. Sub-grain formation in S10/32.

Figure 4. Summary of $^{40}Ar/^{39}Ar$ age spectra. A. 5 hydrothermally altered K-feldspar samples (S08/46A, S09/20, S10/32, S11/6, S11/21); B. 4 host rock samples from Senja and Kvaløya (EG, S09/18, S09/22, S11/20); C. 2 host rock samples from Ringvassøya and Vanna (R3, S10/40). Detailed individual age spectra are included in data repository DR3.

Data Repository, supplementary material on analytical procedures (item DR1), $^{40}Ar/^{39}Ar$ data and sample locations (item DR2), and detailed sample $^{40}Ar/^{39}Ar$ age spectra with Cl/K ratios (item DR3), is available online at XXX.

Table 1 $^{40}Ar/^{39}Ar$ K-feldspar Results

Sample	Lat, Long	Integrated Age (Ma)	Plateau Age (Ma)	Plateau Information	Isochron Age (Ma)	Isochron or other Information
S09/20 (deformed)	69.12052˚N, 17.30883˚E	313.8 ± 1.3	**260.6 ± 1.6***	11 out of 17 fractions 50.1% ^{39}Ar release MSWD = 2.88	--	--
S11/21 (deformed)	69.28062˚N, 17.10295˚E	245.0 ± 1.2	**244.2 ± 1.2**	13 out of 15 fractions 56.8% ^{39}Ar release MSWD = 1.09	--	--
S11/6 (deformed)	69.36030˚N, 17.46383˚E	248.4 ± 0.9	**259.5 ± 1.4***	5 out of 14 fractions 31.6% ^{39}Ar release MSWD = 1.12	261.3 ± 2.8	5 of 14 fractions $^{40}Ar/^{36}Ar_i$ = 274.9 ± 28.3 MSWD = 1.29
S10/32 (deformed)	69.66078˚N, 18.08980˚E	267.4 ± 1.1	**259.2 ± 1.5**	10 out of 14 fractions 58.6% ^{39}Ar release MSWD = 1.42	255.8 ± 2.9	10 of 14 fractions $^{40}Ar/^{36}Ar_i$ = 320.3 ± 22.7 MSWD = 1.30
S08/46 (deformed)	69.72904˚N, 18.32058˚E	261.1 ± 0.9	**264.9 ± 1.2**	6 out of 14 fractions 49.5% ^{39}Ar release MSWD = 1.70	--	--
S11/20 (undeformed)	69.28062˚N, 17.10295˚E	325.4 ± 1.1	--	--	--	--
S09/18 (undeformed)	69.47225˚N, 17.23075˚E	459.7 ± 1.7	--	--	--	--
S09/22 (undeformed)	69.35660˚N, 18.06627˚E	485.4 ± 1.6				
EG (undeformed)	69.70094˚N, 18.60005˚E	451.6 ± 1.5	--	--	--	--
R3 (undeformed)	*70.05195˚N, 19.03317˚E*	421.9 ± 1.5			--	--
S10/40 (undeformed)	70.21555˚N, 19.69545˚E	515.6 ± 1.7			--	--

Samples analyzed with standard MMhb-1 with an age of 523.1 Ma.
Most robust age determination in **bold**.
*Did not meet all the criteria for a plateau age, hence a weighted average age determination is presented.
Coordinate system: WGS84

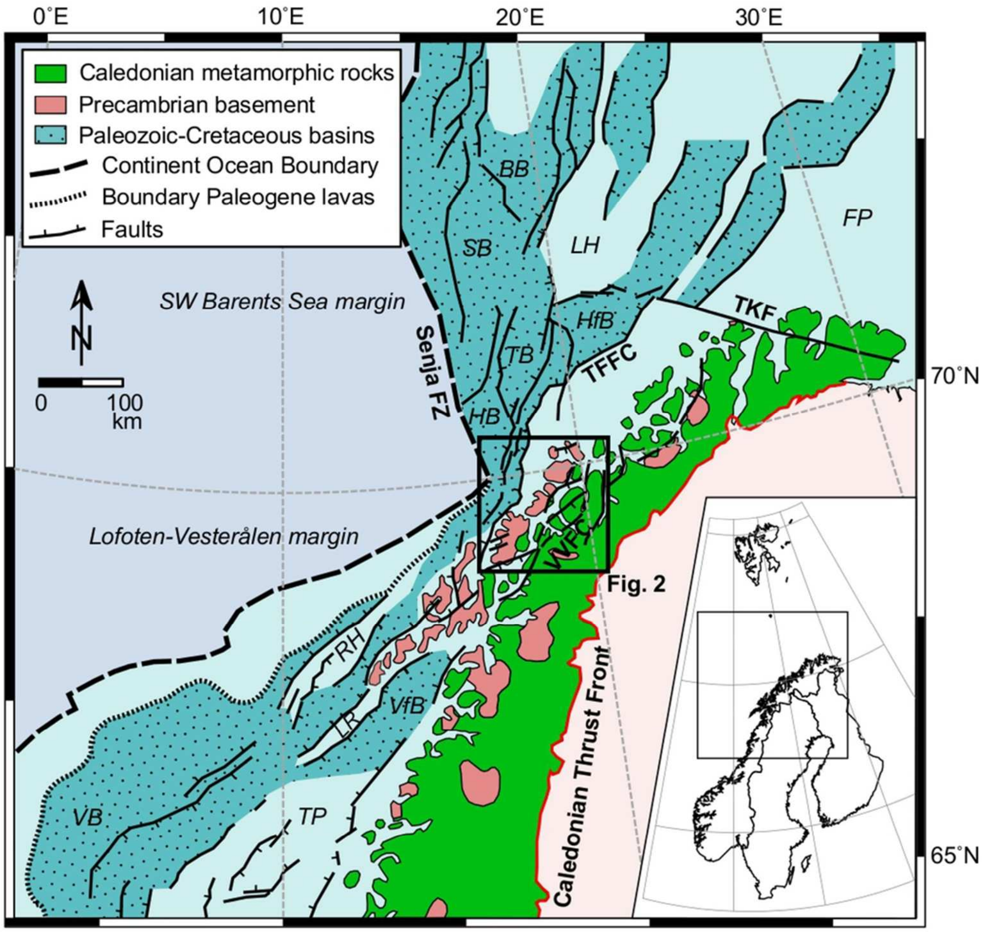

Figure 1. Geological overview map of the North Norwegian margin. Simplified after Mosar et al., (2002) and Faleide et al., (2008). BB: Bjørnøya Basin; FP: Finmark Platform; HB: Harstad Basin; HfB: Hammerfest Basin; LH: Loppa High; LR: Lofoten Ridge; RH: Røst High; SB: Sørvestsnaget Basin; TB: Tromsø Basin; TKF: Trollfjord-Komagelv Fault; TP: Trøndelag Platform; TFFC: Troms-Finmark Fault Complex; VB: Vøring Basin; VfB: Vestfjorden Basin; VVFC: Vestfjorden-Vanna Fault Complex.

86x82mm (300 x 300 DPI)

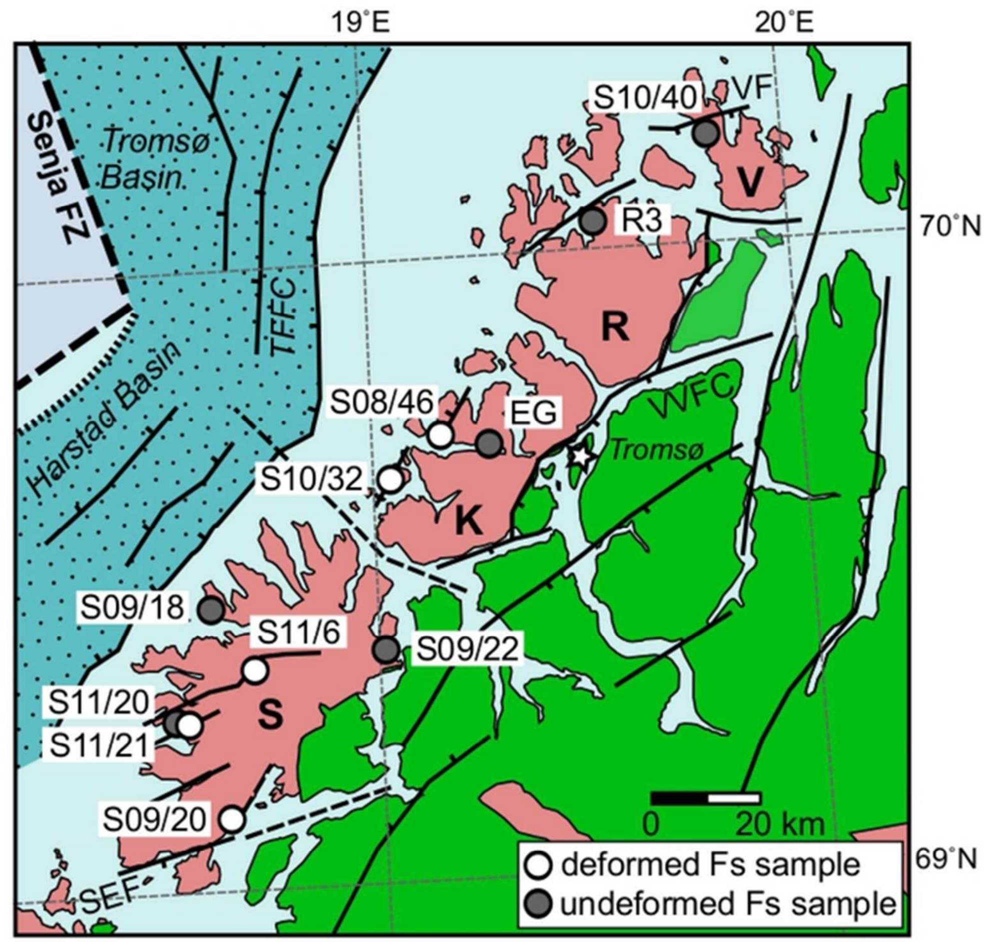

Figure 2. Simplified map of the sample area with sample locations. Fs: K-feldspar; SEF: Stongelandseidet Fault; TFFC: Troms-Finmark Fault Complex; VF: Vannareid Fault; VVFC: Vestfjorden-Vanna Fault Complex. K: Kvaløya; S: Senja; R: Ringvassøya; V: Vanna.

58x56mm (300 x 300 DPI)

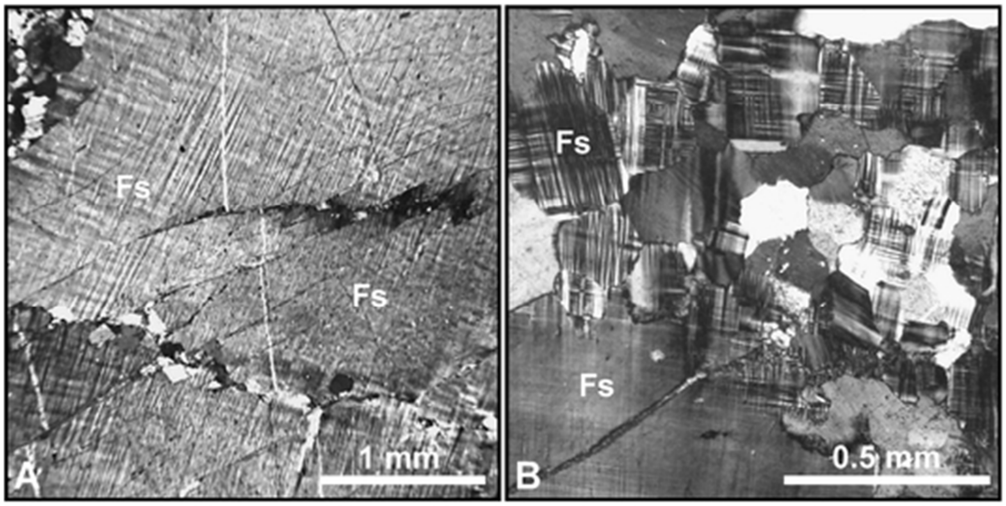

Figure 3. Representative photomicrographs of K-feldspar (KS) from hydrothermally altered fault rocks. A. Microfractures in S08/46A. B. Sub-grain formation in S10/32.

45x22mm (300 x 300 DPI)

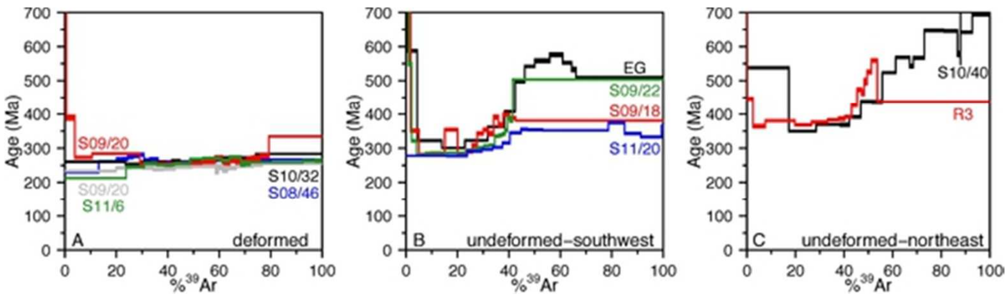

Figure 4. Summary of 40Ar/39Ar age spectra. A. 5 hydrothermally altered K-feldspar samples (S08/46A, S09/20, S10/32, S11/6, S11/21); B. 4 host rock samples from Senja and Kvaløya (EG, S09/18, S09/22, S11/20); C. 2 host rock samples from Ringvassøya and Vanna (R3, S10/40). Detailed individual age spectra are included in data repository DR3.

50x14mm (300 x 300 DPI)

Terra Nova data repository for '*Direct $^{40}Ar/^{39}Ar$ K-feldspar dating of Late Permian - Early Triassic brittle faulting in northern Norway*'

by

Corine Davids[1,2], Jeff A. Benowitz[3*], Paul W. Layer[4], Steffen G. Bergh[2]

[1]Norut Northern Research Institute, NO-9294 Tromsø, Norway

[2]Department of Geosciences, UiT The Arctic University of Norway, NO-9037 Tromsø, Norway

[3]Corresponding author: Geophysical Institute, University of Alaska Fairbanks, Fairbanks, AK 99775-5940, USA, jbenowitz@alaska.edu, 907-474-7010*

[4]College of Natural Science and Mathematics, University of Alaska Fairbanks, Fairbanks, AK 99775-5940, USA

Data Repository (DR) item 1: Analytical procedures.

$^{40}Ar/^{39}Ar$ Analysis

The rock samples were crushed, washed and sieved. Mineral concentrates of K-feldspar were obtained using standard mineral separation procedures, including heavy liquid and magnetic separation. In addition, aliquots of K-feldspar separates derived from the heavy liquid separation were analyzed at the University of Alaska Fairbanks using a Niton xl3t hand held X-ray fluorometer (XRF) to confirm mineral identification and purity. The monitor mineral MMhb-1 (Samson and Alexander, 1987) with an age of 523.1 Ma (Renne et al., 1998) was used to monitor neutron flux and calculate the irradiation parameter J. The samples and standards were wrapped in aluminum foil and loaded into aluminum cans of 2.5 cm diameter and 6 cm height. The samples were irradiated in position 5c of the uranium enriched research reactor of McMaster University in Hamilton, Ontario, Canada for 10 megawatt-hours. Upon their return from the reactor, single K-feldspar grains of the samples and monitors were loaded into 2 mm diameter holes in a copper tray that was then loaded in a ultra-high vacuum extraction line. The monitors were fused and samples step-wise heated, using a 6-watt argon-ion laser following the technique described in York et al. (1981), Layer (2000) and Benowitz et al. (2014). Argon purification was achieved using a liquid nitrogen cold trap and a SAES Zr-Al getter at 400˚C. The samples were analyzed in a VG-3600 mass spectrometer at the Geophysical Institute, University of Alaska Fairbanks. The argon isotopes measured were corrected for system blank and mass discrimination, as well as calcium, potassium and chlorine interference reactions following procedures outlined in McDougall and Harrison (1999). Typical full-system 8 min laser blank values (in moles) were generally 2×10^{-16} mol ^{40}Ar, 3×10^{-18} mol ^{39}Ar, 9×10^{-18} mol ^{38}Ar and 2×10^{-18} mol ^{36}Ar, which are 10–50 times smaller than the sample/standard volume fractions. Correction factors for nucleogenic interferences during irradiation were determined from irradiated CaF_2 and K_2SO_4 as follows: $(^{39}Ar/^{37}Ar)_{Ca} = 7.06 \times 10^{-4}$, $(^{36}Ar/^{37}Ar)_{Ca} = 2.79 \times 10^{-4}$ and $(^{40}Ar/^{39}Ar)_K =$ 0.0297. Mass discrimination was monitored by running calibrated air shots. The mass discrimination during these experiments was 1.3% per mass unit. While doing our experiments, calibration measurements were made on a weekly– monthly basis to check for changes in mass discrimination with no significant variation seen during these intervals. The $^{40}Ar/^{39}Ar$ results are given in Appendix 2, with all ages quoted at the ± 1 sigma level and calculated using the constants of Steiger and Jaeger (1977).

The integrated age is the age given by the total gas measured and is equivalent to a potassium-argon (K-Ar) age if no ^{39}Ar recoil is present.

K-feldspar laser-step heating interpretation

Multidomain diffusion modeling (MDD) K-feldspar thermochronology has proven to be a useful tool in examining orogenic development because of the wide Ar closure-temperature window (ca. 150–350˚C) of the system (McDougall & Harrison, 1999, and references therein). In our study, the age spectra of the brittle K-feldspar are consistently flat as a result of fast cooling, which limits the applicability of MDD modeling. Some of the host rock K-feldspar show intermediate age maxima, indicating problematic behavior that is possibly caused by low temperature alteration (Lovera et al., 2002; Harrison et al., 2005). Inverse modeling may therefore produce incorrect thermal histories. Additionally, during our laser step heating anaylsis the temperature of heating steps is not known, hence MDD modeling is not possible.

For this study, we preferred to use a modified MDD concept approach by analyzing the samples with a more time efficient laser step-heating approach (Benowitz et al., 2011, 2012; Löbens et al., 2017). We examine the resulting age spectra using the MDD approach to determine thermal histories as done by others (Copeland and Harrison, 1990; Ridgway et al., 2007; Benowitz et al., 2014; Riccio et al., 2014).

REFERENCES CITED

Benowitz, J., Layer, P.W., and VanLaningham, S., 2014, Persistent Long-Term (~24 Ma) Exhumation in the Eastern Alaska Range Constrained by Stacked Thermochronology, Geological Society of London Special Volume, 40Ar/39Ar

Dating: from Geochronology to Thermochronology, from Archaeology to Planetary Sciences.

Benowitz, J. A., P. J. Haeussler, P. W. Layer, P. B. O'Sullivan, W. K. Wallace and R. J. Gillis, 2012, Cenozoic tectono-thermal history of the Tordrillo Mountains, Alaska: Paleocene-Eocene ridge subduction, decreasing relief, and late Neogene faulting, Geochemistry, Geophysics, Geosystems, v. 13, Q04009, doi:10.1029/2011GC003951.

Benowitz, J., P. Layer, P. Armstrong, S. Perry, P. Haeussler, P. Fitzgerald, and S. VanLaningham, 2011, Spatial Variations in Focused Exhumation Along a Continental-Scale Strike- Slip Fault: the Denali Fault of the Eastern Alaska Range, Geosphere, v. 7; no. 2; p. 455 467; DOI: 10.1130/GES00589.1

Copeland, P., and Harrison, T.M., 1990, Episodic rapid uplift in the Himalaya revealed by ^{40}Ar/^{39}Ar analysis of detrital K-feldspar and muscovite, Bengal fan, Geology, v. 18, 354–357, doi:10.1130/0091-7613(1990)018<0354:ERUITH>2.3.CO;2.

Harrison, T.M., Grove, M., Lovera, O.M., and Zeitler, P.K., 2005, Continuous Thermal Histoties from Inversion of Closure Profiles, *in* Reiners,. P.W. and Ehlers, T.A., eds., Low-Temperature Thermochronology, Techniques, Interpretations, and Applications: Reviews in Mineralogy and Geochemistry, v. 58, p. 389–409**.**

Layer, P.W., 2000, 40Ar/39Ar age of the El'gygytgyn impact event, Chukotka, Russia: Meteoritics & Planetary Science, v. 35, p. 591–599.

Löbens, S., Oriolo, S., Benowitz, J., Wemmer, K., Layer,P., Siegesmund,S., 2017, Late Paleozoic deformation and exhumation in the Sierras Pampeanas (Argentina): constrained by first Ar/Ar-feldspar datings, International Journal of Earth Science.

Lovera, O. M., Grove, M., and Harrison, T.M., 2002, Systematic analysis of K-feldspar ^{40}Ar/^{39}Ar step heating results: II. Relevance of laboratory argon diffusion properties to nature, Geochimica et Cosmochimica Acta, 66, 1237–1255, doi:10.1016/ S0016-7037(01)00846-8.

McDougall, I., and Harrison, T.M., 1999, Geochronology and Thermochronologv by the 40Ar/39Ar Method: New York, USA, Oxford University Press, 288 p.

Renne, P.R., Swisher, C.C., Deino, A.L., Karner, D.B., Owens, T.L., and DePaolo, D.J., 1998, Intercalibration of standards, absolute ages and uncertainties in ^{40}Ar/^{39}Ar dating: Chemical Geology, v. 145, p. 117–152.

Riccio, S. J., Fitzgerald, P.G., Benowitz, J.A., and Roeske, S.M.,2014, The role of thrust faulting in the formation of the eastern Alaska Range Thermochronological constraints from the Susitna Glacier Thrust Fault region of the intracontinental strike-slip Denali Fault system: Tectonics, v. 33, p. 2195-2217, doi: 10.1002/2014TC003646, 2014.

Ridgway, K. D., Thoms, E.E., Layer, P.W., Lesh, M.E., White, J.M., and Smith, S.V., 2007, Neogene transpressional foreland basin development on the north side of the central Alaska Range, Usibelli Group and Nenana Gravel, Tanana basin, in Tectonic Growth of a Collisional Continental Margin: Crustal Evolution of Southern Alaska, edited by K. D. Ridgway et al., Spec. Pap. Geol. Soc. Am., 431, 507–547, doi:10.1130/ 2007.2431(20).

Samson, S.D., and Alexander, E.C., 1987, Calibration of the interlaboratory ^{40}Ar-^{39}Ar dating standard, MMhb-1: Chemical Geology, v. 66, p. 27–34.

Steiger, R.H., and Jaeger, E., 1977, Subcommission on geochronology: Convention on the use of decay constants in geo and cosmochronology: Earth and Planetary Science Letters, v. 36, p. 359–362.

York, D., Hall, C.M., Yanase, Y., Hanes, J.A., and Kenyon, W.J., 1981, 40Ar/39Ar dating of terrestrial minerals with a continuous laser: Geophysical Research Letters, v. 8, p. 1136–11.

DR item 2: $^{40}Ar/^{39}Ar$ data and sample locations.

FS= Potassium Feldspar
L=Laser
9001 Step: Same power as 9000 mW step, but with the laser spot focused down to assure fusion.

Sample name: S08/46A FS#L1 (deformed)
Location: Rekvika, Kvaløya (69.72904˚N, 18.32058˚E)
Weighted average of J from standards = 3.652e-03 +/- 1.134e-05
Days since irradiation = 33

Laser Power (mW)	Cumulative 39Ar	40Ar/39Ar meas.	+/-	37Ar/39Ar meas.	+/-	36Ar/39Ar meas.	+/-	% Atm. 40Ar	+/-	Ca/K	+/-	Cl/K	+/-	40*/39K	+/-	Age (Ma)	+/- (Ma)
400	0.1314	43.8438	0.2803	0.0031	0.0006	0.0225	0.0004	15.1394	0.2595	0.0056	0.0010	0.0012	0.0001	37.1810	0.2834	229.73	1.64
600	0.2011	43.4093	0.2381	0.0041	0.0008	0.0019	0.0004	1.2763	0.2646	0.0075	0.0015	0.0003	0.0001	42.8260	0.2626	262.18	1.5
800	0.2261	44.5501	0.3148	0.0330	0.0039	0.0014	0.0012	0.8926	0.8114	0.0605	0.0071	0.0007	0.0003	44.1240	0.4776	269.56	2.71
1000	0.2441	44.6529	0.4228	0.1492	0.0056	0.0024	0.0021	1.5861	1.3899	0.2738	0.0102	0.0009	0.0003	43.9200	0.7482	268.4	4.25
1300	0.2649	45.5575	0.4612	0.2358	0.0055	0.0023	0.0015	1.4445	0.9683	0.4326	0.0101	0.0011	0.0003	44.8777	0.6344	273.83	3.59
1600	0.2849	45.2195	0.4144	0.0309	0.0045	-0.0020	0.0027	-1.2800	1.7360	0.0567	0.0083	0.0011	0.0003	45.7692	0.8888	278.87	5.02
2000	0.3069	46.9655	0.4444	0.0406	0.0065	0.0023	0.0018	1.4114	1.1098	0.0745	0.0119	0.0001	0.0011	46.2747	0.6816	281.72	3.84
2500	0.3309	47.1545	0.4278	0.0250	0.0038	0.0123	0.0012	7.7090	0.7368	0.0458	0.0070	0.0015	0.0002	43.4927	0.5312	265.97	3.02
3000	0.3618	49.1021	0.2527	0.0067	0.0023	0.0166	0.0012	9.9856	0.7453	0.0123	0.0041	0.0023	0.0003	44.1724	0.4327	269.83	2.45
4000	0.5676	47.5981	0.0895	0.0018	0.0004	0.0152	0.0003	9.4118	0.1930	0.0034	0.0008	0.0017	0.0001	43.0914	0.1247	263.69	0.71
5000	0.7428	47.8179	0.1095	0.0005	0.0005	0.0152	0.0002	9.4218	0.1052	0.0010	0.0009	0.0018	0.0001	43.2857	0.1137	264.8	0.65
6000	0.7854	48.9381	0.1701	-0.0011	0.0016	0.0179	0.0007	10.8291	0.4139	-0.0021	0.0029	0.0024	0.0002	43.6120	0.2556	266.65	1.45
9000	0.8014	49.3682	0.4330	0.0000	0.0048	0.0207	0.0022	12.3898	1.3304	0.0000	0.0088	0.0019	0.0004	43.2255	0.7693	264.45	4.38
9001	1.0000	49.2209	0.1311	0.0003	0.0004	0.0175	0.0003	10.5100	0.1774	0.0006	0.0007	0.0020	0.0001	44.0213	0.1484	268.98	0.84
Integrated		47.0618	0.0611	0.0119	0.0003	0.0144	0.0002	9.0330	0.0966	0.0218	0.0006	0.0016	0.0000	42.7841	0.0733	261.94	0.86

Sample: S09/20 FS#L1 (deformed)
Location: Vassvik, Senja (69.12052˚N, 17.30883˚E)
Weighted average of J from standards = 3.775e-03 +/- 1.217e-05
Days since irradiation = 62

Laser Power (mW)	Cumulative 39Ar	40Ar/39Ar meas.	+/-	37Ar/39Ar meas.	+/-	36Ar/39Ar meas.	+/-	% Atm. 40Ar	+/-	Ca/K	+/-	Cl/K	+/-	40*/39K	+/-	Age (Ma)	+/- (Ma)
400	0.0013	2658.5766	#####	0.0761	0.2029	0.4511	0.0781	5.0138	0.7806	0.1397	0.3724	0.0907	0.0111	2525.3888	193.4282	4245	124.9
600	0.0063	405.7988	8.3351	0.0319	0.0662	0.0605	0.0190	4.4037	1.3773	0.0585	0.1215	0.0097	0.0022	387.9089	9.7521	1626.7	26.93
800	0.0384	66.1839	0.6711	0.0037	0.0102	0.0079	0.0038	3.5100	1.7061	0.0069	0.0187	0.0013	0.0003	63.8323	1.3034	389.48	7.15
1000	0.1054	43.9583	0.2242	0.0022	0.0050	0.0022	0.0015	1.4900	1.0343	0.0040	0.0092	0.0006	0.0002	43.2742	0.5057	272.99	2.96
1300	0.2922	46.0665	0.3010	-0.0002	0.0016	0.0027	0.0005	1.7064	0.2954	-0.0003	0.0029	0.0007	0.0001	45.2512	0.3275	284.52	1.91
1600	0.4315	40.7964	0.2779	0.0015	0.0021	0.0019	0.0008	1.3772	0.5404	0.0028	0.0039	0.0004	0.0001	40.2052	0.3527	254.93	2.09
1900	0.5316	41.0781	0.2956	0.0033	0.0025	0.0021	0.0009	1.5334	0.6576	0.0061	0.0046	0.0004	0.0001	40.4190	0.3983	256.19	2.35
2200	0.5838	41.7089	0.3455	0.0079	0.0079	0.0023	0.0023	1.5930	1.6046	0.0144	0.0145	0.0008	0.0002	41.0155	0.7508	259.72	4.43
2500	0.6119	43.2499	0.4456	0.0068	0.0103	0.0003	0.0029	0.1825	1.9847	0.0125	0.0189	0.0010	0.0004	43.1416	0.9663	272.21	5.66
3000	0.6410	42.1296	0.3016	0.0124	0.0136	0.0048	0.0034	3.3328	2.3573	0.0227	0.0250	0.0008	0.0003	40.6971	1.0351	257.84	6.11
3500	0.6648	42.1012	0.2566	0.0059	0.0114	-0.0001	0.0040	-0.0596	2.8214	0.0108	0.0209	0.0011	0.0006	42.0968	1.2145	266.08	7.14
4000	0.6856	42.1318	0.5064	0.0065	0.0125	0.0026	0.0045	1.8280	3.1435	0.0119	0.0229	0.0011	0.0008	41.3326	1.4140	261.58	8.33
4500	0.7069	42.6240	0.5085	0.0002	0.0124	0.0073	0.0049	5.0495	3.4238	0.0004	0.0227	0.0006	0.0006	40.4435	1.5369	256.34	9.08
5000	0.7279	42.9368	0.2718	0.0075	0.0150	0.0028	0.0041	1.9241	2.8041	0.0137	0.0276	0.0011	0.0005	42.0818	1.2325	265.99	7.24
6000	0.7582	44.3274	0.3808	0.0135	0.0077	0.0052	0.0040	3.4675	2.6711	0.0248	0.0142	0.0006	0.0003	42.7621	1.2397	269.99	7.27
9000	0.7930	45.0823	0.4266	0.0096	0.0072	0.0034	0.0027	2.2323	1.7665	0.0176	0.0132	0.0006	0.0003	44.0472	0.8992	277.51	5.25
9001	1.0000	55.4887	0.2305	0.0000	0.0016	0.0048	0.0003	2.5506	0.1661	0.0000	0.0030	0.0006	0.0001	54.0444	0.2433	334.95	1.38
Integrated		51.5505	0.1071	0.0032	0.0013	0.0040	0.0004	2.3179	0.2316	0.0058	0.0023	0.0008	0.0001	50.3267	0.1591	313.8	1.3

Sample name: S10/32 FS#L1 (deformed)
Location: Tussøya (69.66078˚N, 18.08980˚E)
Weighted average of J from standards = 3.688e-03 +/- 1.087e-05
Days since irradiation = 37

Laser Power (mW)	Cumulative 39Ar	40Ar/39Ar meas.	+/-	37Ar/39Ar meas.	+/-	36Ar/39Ar meas.	+/-	% Atm. 40Ar	+/-	Ca/K	+/-	Cl/K	+/-	40*/39K	+/-	Age (Ma)	+/- (Ma)
400	0.2355	48.7776	0.3153	0.0044	0.0004	0.0224	0.0006	13.5510	0.3713	0.0082	0.0007	0.0033	0.0001	42.1423	0.3307	260.66	1.9
600	0.2925	42.2726	0.3058	0.0535	0.0034	0.0046	0.0012	3.1904	0.8292	0.0982	0.0062	0.0003	0.0002	40.8967	0.4608	253.48	2.66
800	0.3293	43.1927	0.2575	0.0296	0.0037	0.0046	0.0014	3.1158	0.9273	0.0543	0.0068	0.0005	0.0002	41.8190	0.4737	258.8	2.73
1000	0.3586	44.8633	0.3486	0.0148	0.0045	0.0116	0.0026	7.6138	1.7426	0.0272	0.0083	0.0006	0.0004	41.4205	0.8483	256.5	4.9
1300	0.3913	50.2834	0.4418	0.0371	0.0023	0.0292	0.0019	17.1413	1.1123	0.0680	0.0043	0.0014	0.0003	41.6407	0.6753	257.77	3.9
1600	0.4155	51.3586	0.3756	0.0260	0.0068	0.0362	0.0023	20.8273	1.3182	0.0477	0.0125	0.0026	0.0004	40.6392	0.7476	251.99	4.33
2000	0.4469	51.3470	0.4777	0.0163	0.0024	0.0306	0.0028	17.6122	1.6173	0.0298	0.0044	0.0023	0.0004	42.2797	0.9261	261.45	5.33
2500	0.5031	49.7961	0.3787	0.0088	0.0017	0.0283	0.0015	16.7946	0.8754	0.0161	0.0031	0.0020	0.0003	41.4086	0.5469	256.43	3.16
3000	0.5335	49.8197	0.3651	0.0171	0.0031	0.0258	0.0025	15.3232	1.4890	0.0315	0.0056	0.0025	0.0003	42.1611	0.8101	260.77	4.67
3500	0.5864	50.8779	0.4769	0.0111	0.0019	0.0266	0.0015	15.4677	0.8730	0.0203	0.0035	0.0035	0.0002	42.9835	0.6104	265.5	3.51
4000	0.7405	51.3152	0.4302	0.0048	0.0005	0.0242	0.0006	13.9626	0.3335	0.0088	0.0009	0.0023	0.0001	44.1248	0.4292	272.04	2.46
9000	1.0000	54.2543	0.2746	0.0056	0.0007	0.0276	0.0004	15.0142	0.2271	0.0102	0.0012	0.0026	0.0001	46.0834	0.2697	283.22	1.53
Integrated		50.2911	0.1301	0.0118	0.0004	0.0235	0.0003	13.8080	0.1736	0.0216	0.0008	0.0024	0.0001	43.3217	0.1451	267.44	1.11

Late Permian - Early Triassic Northern Norway Faulting

Sample name: S11/6 FS#L1 (deformed)
Location: Heggdalen, Senja (69.36030˚N, 17.46383˚E)
Weighted average of J from standards = 3.688e-03 +/- 1.087e-05
Days since irradiation = 38

Laser Power (mW)	Cumulative 39Ar	40Ar/39Ar meas.	+/-	37Ar/39Ar meas.	+/-	36Ar/39Ar meas.	+/-	% Atm. 40Ar	+/-	Ca/K	+/-	Cl/K	+/-	40*/39K	+/-	Age (Ma)	+/- (Ma)
400	0.2381	36.6789	0.1873	0.0309	0.0008	0.0094	0.0002	7.5415	0.1737	0.0567	0.0014	0.0010	0.0001	33.8861	0.1861	212.48	1.1
600	0.3088	41.5399	0.2693	0.0969	0.0022	0.0068	0.0006	4.8058	0.4484	0.1777	0.0041	0.0020	0.0002	39.5180	0.3221	245.49	1.87
800	0.3558	44.5417	0.4320	0.0728	0.0031	0.0113	0.0008	7.5074	0.5375	0.1335	0.0057	0.0020	0.0003	41.1724	0.4708	255.07	2.72
1000	0.4252	43.3823	0.2912	0.0543	0.0025	0.0098	0.0010	6.6622	0.6769	0.0996	0.0046	0.0021	0.0002	40.4659	0.4049	250.98	2.34
1300	0.4864	43.9941	0.3032	0.0460	0.0021	0.0096	0.0008	6.4260	0.5019	0.0844	0.0039	0.0018	0.0002	41.1406	0.3651	254.89	2.11
1600	0.5365	46.8599	0.3754	0.0517	0.0023	0.0114	0.0008	7.2026	0.4689	0.0949	0.0042	0.0015	0.0002	43.4588	0.4175	268.23	2.39
2000	0.6025	46.8332	0.3532	0.0455	0.0019	0.0096	0.0007	6.0683	0.4678	0.0835	0.0035	0.0017	0.0002	43.9647	0.4038	271.13	2.31
2500	0.6395	46.0486	0.3464	0.0438	0.0027	0.0109	0.0014	6.9664	0.9131	0.0803	0.0050	0.0017	0.0003	42.8144	0.5341	264.53	3.07
3000	0.6838	55.4916	0.3544	0.1552	0.0032	0.0369	0.0016	19.6244	0.8230	0.2848	0.0059	0.0026	0.0003	44.5827	0.5556	274.66	3.17
3500	0.6989	55.9577	0.4054	0.2661	0.0084	0.0500	0.0037	26.4006	1.9278	0.4884	0.0155	0.0045	0.0007	41.1704	1.1289	255.06	6.52
4000	0.7200	49.6350	0.4024	0.1469	0.0063	0.0282	0.0029	16.7593	1.7014	0.2696	0.0115	0.0032	0.0005	41.2961	0.9132	255.78	5.27
5000	0.9247	45.6290	0.2136	0.0445	0.0007	0.0128	0.0003	8.3048	0.1622	0.0816	0.0012	0.0018	0.0001	41.8137	0.2118	258.77	1.22
6000	0.9733	45.1526	0.3887	0.0283	0.0025	0.0085	0.0009	5.5856	0.5524	0.0520	0.0045	0.0014	0.0002	42.6034	0.4475	263.32	2.57
9001	1.0000	49.3338	0.5591	0.0189	0.0039	0.0226	0.0017	13.5355	0.9939	0.0346	0.0071	0.0016	0.0003	42.6312	0.7102	263.48	4.08
Integrated		43.8119	0.0886	0.0564	0.0005	0.0127	0.0002	8.5909	0.1299	0.1035	0.0010	0.0017	0.0000	40.0225	0.1003	248.41	0.9

Sample name: S11/21 FS#L1 (deformed)
Location: Sifjord, Senja (69.28062˚N, 17.10295˚E)
Weighted average of J from standards = 3.688e-03 +/- 1.087e-05
Days since irradiation = 38

Laser Power (mW)	Cumulative 39Ar	40Ar/39Ar meas.	+/-	37Ar/39Ar meas.	+/-	36Ar/39Ar meas.	+/-	% Atm. 40Ar	+/-	Ca/K	+/-	Cl/K	+/-	40*/39K	+/-	Age (Ma)	+/- (Ma)
400	0.1988	38.5487	0.3076	0.0045	s10/40	0.0036	0.0004	2.7520	0.3389	0.0082	0.0017	0.0007	0.0001	37.4591	0.3303	233.49	1.93
600	0.2574	39.4889	0.3685	0.0163	0.0024	0.0014	0.0012	1.0341	0.8897	0.0300	0.0044	0.0006	0.0002	39.0516	0.5068	242.78	2.95
800	0.3028	39.4802	0.3134	0.0086	0.0025	0.0005	0.0014	0.3366	1.0122	0.0158	0.0045	0.0007	0.0005	39.3179	0.5071	244.33	2.95
1000	0.3428	39.5967	0.4119	0.0066	0.0032	0.0015	0.0020	1.0997	1.4768	0.0120	0.0058	0.0007	0.0004	39.1321	0.7128	243.25	4.14
1300	0.3813	39.4353	0.3189	0.0069	0.0029	0.0037	0.0018	2.8037	1.3094	0.0127	0.0053	0.0008	0.0004	38.3010	0.6031	238.41	3.52
1600	0.4280	39.4360	0.3868	0.0094	0.0025	0.0029	0.0013	2.1947	0.9940	0.0173	0.0046	0.0014	0.0003	38.5417	0.5456	239.81	3.18
2000	0.4939	40.2920	0.3052	0.0046	0.0020	0.0029	0.0011	2.1038	0.8184	0.0084	0.0037	0.0010	0.0002	39.4154	0.4463	244.89	2.59
2500	0.5849	40.8294	0.2667	0.0032	0.0014	0.0035	0.0009	2.5427	0.6575	0.0058	0.0025	0.0012	0.0002	39.7624	0.3751	246.91	2.18
3000	0.5957	40.0382	0.5608	0.0259	0.0111	0.0053	0.0077	3.9126	5.6470	0.0476	0.0203	0.0013	0.0012	38.4439	2.3231	239.24	13.54
3500	0.6139	40.5749	0.4506	0.0115	0.0067	0.0039	0.0036	2.8089	2.6562	0.0211	0.0122	0.0011	0.0007	39.4067	1.1631	244.84	6.76
4000	0.6313	41.0240	0.4383	0.0170	0.0076	0.0094	0.0044	6.8017	3.1836	0.0311	0.0140	0.0003	0.0008	38.2064	1.3693	237.85	7.99
5000	0.6652	40.4798	0.4240	0.0022	0.0037	0.0049	0.0022	3.6094	1.5845	0.0040	0.0068	0.0009	0.0004	38.9902	0.7617	242.42	4.43
6000	0.7310	40.9681	0.3361	0.0018	0.0017	0.0036	0.0011	2.5783	0.7829	0.0033	0.0032	0.0011	0.0002	39.8829	0.4598	247.61	2.67
9000	0.7667	41.8415	0.2347	0.0048	0.0035	0.0043	0.0020	3.0434	1.3779	0.0088	0.0064	0.0006	0.0005	40.5394	0.6208	251.41	3.59
9001	1.0000	42.5937	0.5515	-0.0019	0.0006	0.0038	0.0004	2.6347	0.2739	-0.0036	0.0011	0.0005	0.0001	41.4425	0.5545	256.63	3.2
Integrated		40.4680	0.1511	0.0045	0.0005	0.0034	0.0003	2.4815	0.2118	0.0083	0.0009	0.0008	0.0001	39.4350	0.1716	245.01	1.2

Sample name: EG FS#L2 (undeformed)
Location: Ersfjordbotn, Kvaløya (69.70094˚N, 18.60005˚E)
Weighted average of J from standards = 3.657e-03e-03 +/- 1.135e-05
Days since irradiation = 166

Laser Power (mW)	Cumulative 39Ar	40Ar/39Ar meas.	+/-	37Ar/39Ar meas.	+/-	36Ar/39Ar meas.	+/-	% Atm. 40Ar	+/-	Ca/K	+/-	Cl/K	+/-	40*/39K	+/-	Age (Ma)	+/- (Ma)
400	0.0032	238.3138	5.4156	-0.3789	0.2469	0.1577	0.0113	19.5658	1.3663	-0.6950	0.4527	0.0071	0.0024	191.6106	5.6405	956.94	21.86
600	0.0432	105.8832	0.6841	-0.0609	0.0253	0.0013	0.0006	0.3702	0.1710	-0.1117	0.0464	0.0017	0.0002	105.4571	0.7055	587.75	3.36
800	0.1392	53.7277	0.4679	-0.0256	0.0095	0.0004	0.0003	0.2396	0.1755	-0.0469	0.0173	0.0007	0.0001	53.5683	0.4766	322.37	2.63
1000	0.2291	49.9157	0.2583	-0.0044	0.0089	0.0007	0.0004	0.3949	0.2164	-0.0080	0.0163	0.0003	0.0001	49.6889	0.2794	300.86	1.56
1300	0.3175	53.8212	0.3544	-0.0067	0.0123	0.0005	0.0005	0.2677	0.2657	-0.0123	0.0225	0.0006	0.0001	53.6472	0.3815	322.8	2.1
1600	0.3833	61.3392	0.2148	0.0566	0.0248	0.0013	0.0007	0.6218	0.3263	0.1039	0.0456	0.0005	0.0002	60.9307	0.2929	362.49	1.58
2000	0.4237	69.8814	0.3659	-0.0089	0.0279	0.0018	0.0009	0.7398	0.3721	-0.0163	0.0512	0.0006	0.0002	69.3346	0.4471	407.22	2.35
2500	0.4612	87.1108	0.4176	0.0085	0.0342	0.0013	0.0013	0.4240	0.4248	0.0156	0.0628	0.0007	0.0002	86.7124	0.5568	496.33	2.79
3000	0.5004	96.6901	0.4966	0.0119	0.0382	0.0024	0.0012	0.7292	0.3698	0.0219	0.0700	0.0013	0.0003	95.9564	0.6092	542	2.97
4000	0.5589	99.5612	1.0407	-0.0307	0.0279	0.0007	0.0007	0.2026	0.1998	-0.0563	0.0512	0.0011	0.0002	99.3277	1.0582	558.37	5.12
5000	0.6092	103.6549	1.0316	-0.0035	0.0268	0.0020	0.0012	0.5656	0.3274	-0.0064	0.0492	0.0014	0.0002	103.0389	1.0826	576.22	5.18
6000	0.6440	98.8344	0.5490	0.0237	0.0427	0.0026	0.0015	0.7659	0.4561	0.0434	0.0784	0.0014	0.0003	98.0496	0.7076	552.18	3.43
9000	0.6609	96.2039	0.7532	0.0147	0.0744	0.0072	0.0036	2.2049	1.1106	0.0270	0.1366	0.0012	0.0004	94.0546	1.2995	532.69	6.37
9001	1.0000	85.5636	0.3173	0.0014	0.0044	0.0012	0.0005	0.4015	0.1842	0.0025	0.0081	0.0008	0.0001	85.1906	0.3532	488.7	1.77
Integrated		78.4325	0.1510	-0.0034	0.0048	0.0017	0.0002	0.6565	0.0904	-0.0062	0.0087	0.0009	0.0000	77.8879	0.1661	451.63	1.5

Late Permian - Early Triassic Northern Norway Faulting

Sample name: S09/18 FS#L1 (undeformed)
Location: Bøvær, Senja (69.47225˚N, 17.23075˚E)
Weighted average of J from standards = 3.775e-03 +/- 1.217e-05
Days since irradiation = 62

Laser Power (mW)	Cumulative 39Ar	40Ar/39Ar meas.	+/-	37Ar/39Ar meas.	+/-	36Ar/39Ar meas.	+/-	% Atm. 40Ar	+/-	Ca/K	+/-	Cl/K	+/-	40*/39K	+/-	Age (Ma)	+/- (Ma)
400	0.0035	4940.2824	#####	-0.0408	0.0425	0.1999	0.0135	1.1957	0.0747	-0.0749	0.0779	0.0179	0.0028	4881.0441	124.9137	5348.1	43.75
600	0.0176	150.2900	1.9266	0.0133	0.0124	0.0111	0.0047	2.1847	0.9141	0.0244	0.0228	0.0020	0.0006	146.9789	2.3395	796.18	10.24
800	0.0505	57.8220	0.6146	0.0085	0.0050	0.0027	0.0014	1.3596	0.7232	0.0156	0.0091	0.0006	0.0002	57.0068	0.7384	351.63	4.14
1000	0.0962	45.3610	0.3453	0.0134	0.0042	0.0018	0.0010	1.1735	0.6710	0.0245	0.0077	0.0005	0.0003	44.7998	0.4589	281.89	2.67
1300	0.1509	46.1038	0.3183	0.0104	0.0030	0.0015	0.0009	0.9333	0.5612	0.0191	0.0055	0.0006	0.0001	45.6444	0.4092	286.81	2.38
1600	0.2002	57.9745	0.5369	0.0094	0.0035	0.0016	0.0010	0.8288	0.5065	0.0173	0.0064	0.0005	0.0001	57.4649	0.6092	354.2	3.41
1900	0.2319	44.7847	0.3908	0.0072	0.0056	0.0013	0.0016	0.8772	1.0291	0.0133	0.0103	0.0006	0.0002	44.3627	0.6025	279.35	3.51
2200	0.2574	45.8060	0.2259	0.0107	0.0071	-0.0013	0.0020	-0.8422	1.2764	0.0196	0.0130	0.0006	0.0003	46.1622	0.6267	289.81	3.63
2500	0.2763	48.4218	0.3291	0.0020	0.0091	-0.0032	0.0027	-1.9423	1.6404	0.0036	0.0167	0.0004	0.0003	49.3321	0.8610	308.1	4.94
3000	0.3007	54.7031	0.4353	0.0078	0.0075	-0.0028	0.0022	-1.4892	1.1686	0.0144	0.0138	0.0009	0.0003	55.4879	0.7756	343.1	4.37
3500	0.3203	56.3267	0.4607	0.0166	0.0088	-0.0037	0.0023	-1.9460	1.1896	0.0305	0.0162	0.0010	0.0004	57.3932	0.8168	353.8	4.57
4000	0.3402	54.8169	0.4754	0.0015	0.0088	-0.0021	0.0031	-1.1088	1.6889	0.0028	0.0162	0.0008	0.0004	55.3947	1.0423	342.58	5.87
4500	0.3591	63.4470	0.5302	0.0150	0.0081	-0.0023	0.0029	-1.0870	1.3340	0.0275	0.0149	0.0008	0.0004	64.1073	1.0010	390.99	5.49
5000	0.3776	58.8081	0.4105	0.0104	0.0100	-0.0039	0.0032	-1.9693	1.6170	0.0190	0.0184	0.0008	0.0004	59.9363	1.0376	367.97	5.76
6000	0.4022	65.1560	0.6384	0.0023	0.0066	-0.0010	0.0020	-0.4708	0.9047	0.0043	0.0120	0.0007	0.0003	65.4330	0.8706	398.24	4.75
9000	0.4256	63.2955	0.4513	0.0108	0.0068	-0.0014	0.0022	-0.6480	1.0105	0.0197	0.0125	0.0007	0.0004	63.6763	0.7836	388.62	4.3
9001	1.0000	62.9987	0.2456	0.0044	0.0003	0.0024	0.0001	1.1240	0.0382	0.0080	0.0005	0.0008	0.0000	62.2614	0.2444	380.84	1.35
Integrated		77.5506	0.1844	0.0063	0.0007	0.0022	0.0002	0.8243	0.0810	0.0116	0.0013	0.0008	0.0000	76.8823	0.1936	459.7	1.66

Late Permian - Early Triassic Northern Norway Faulting

Sample name: S09/22 FS#L1 (undeformed)
Location: Gibostad, Senja (69.35660˚N, 18.06627˚E)
Weighted average of J from standards = 3.775e-03 +/- 1.217e-05
Days since irradiation = 63

Laser Power (mW)	Cumulative 39Ar	40Ar/39Ar meas.	+/-	37Ar/39Ar meas.	+/-	36Ar/39Ar meas.	+/-	% Atm. 40Ar	+/-	Ca/K	+/-	Cl/K	+/-	40*/39K	+/-	Age (Ma)	+/- (Ma)
400	0.0101	1170.4346	6.9629	-0.0185	0.0055	0.0675	0.0024	1.7042	0.0597	-0.0340	0.0101	0.0122	0.0003	#####	6.8876	3021.7	8.77
600	0.0220	97.3698	0.7684	0.0021	0.0048	0.0106	0.0019	3.2017	0.5725	0.0039	0.0088	0.0016	0.0002	94.2238	0.9357	548.98	4.7
800	0.0415	53.3069	0.4657	-0.0020	0.0023	0.0052	0.0011	2.8915	0.6157	-0.0036	0.0043	0.0008	0.0001	51.7366	0.5614	321.85	3.2
1000	0.0762	45.5829	0.3025	0.0026	0.0015	0.0032	0.0006	2.1009	0.4068	0.0048	0.0027	0.0006	0.0001	44.5963	0.3521	280.71	2.05
1300	0.1642	46.4820	0.1658	0.0011	0.0006	0.0027	0.0003	1.7393	0.1920	0.0019	0.0012	0.0005	0.0001	45.6444	0.1862	286.81	1.08
1600	0.2375	46.2604	0.1980	0.0006	0.0009	0.0016	0.0004	1.0239	0.2415	0.0011	0.0017	0.0004	0.0001	45.7574	0.2258	287.46	1.31
1900	0.2761	47.7691	0.2822	0.0031	0.0013	0.0019	0.0005	1.1833	0.3176	0.0058	0.0024	0.0004	0.0001	47.1746	0.3189	295.67	1.84
2200	0.3037	48.8519	0.3556	0.0023	0.0016	0.0021	0.0008	1.2668	0.4695	0.0043	0.0029	0.0004	0.0001	48.2038	0.4207	301.61	2.42
2500	0.3256	50.0355	0.3301	-0.0012	0.0025	0.0025	0.0009	1.4936	0.5442	-0.0021	0.0045	0.0004	0.0002	49.2589	0.4256	307.68	2.44
3000	0.3454	50.3244	0.3825	0.0029	0.0034	0.0024	0.0010	1.3988	0.6108	0.0054	0.0062	0.0004	0.0002	49.5913	0.4876	309.59	2.8
3500	0.3620	54.9486	0.4132	0.0024	0.0032	0.0028	0.0014	1.4807	0.7619	0.0044	0.0059	0.0005	0.0002	54.1058	0.5852	335.3	3.31
4000	0.3739	54.7060	0.3909	0.0093	0.0029	0.0003	0.0017	0.1638	0.9246	0.0170	0.0053	0.0003	0.0003	54.5871	0.6387	338.02	3.61
4500	0.3847	56.0886	0.3210	0.0062	0.0047	0.0029	0.0019	1.5006	1.0025	0.0114	0.0086	0.0006	0.0004	55.2179	0.6460	341.58	3.64
5000	0.3941	58.0647	0.3124	-0.0012	0.0060	0.0031	0.0025	1.5650	1.2476	-0.0021	0.0110	0.0000	0.0005	57.1267	0.7877	352.3	4.41
6000	0.4039	64.6130	0.6238	0.0000	0.0067	0.0031	0.0022	1.3965	1.0164	0.0001	0.0122	0.0002	0.0003	63.6814	0.9008	388.65	4.95
9000	0.4142	63.8568	0.6021	0.0030	0.0045	0.0054	0.0020	2.5000	0.9379	0.0056	0.0082	0.0004	0.0003	62.2315	0.8402	380.67	4.63
9001	1.0000	85.9862	0.2755	0.0004	0.0001	0.0023	0.0000	0.7964	0.0152	0.0008	0.0002	0.0011	0.0000	85.2719	0.2741	503.44	1.41
Integrated		82.7515	0.1659	0.0007	0.0002	0.0032	0.0001	1.1308	0.0333	0.0014	0.0004	0.0010	0.0000	81.7864	0.1668	485.4	1.62

Sample name: S11/20 FS#1 (undeformed)
Location: Sifjord, Senja (69.28062˚N, 17.10295˚E)
Weighted average of J from standards = 3.688e-03 +/- 1.087e-05
Days since irradiation = 38

Laser Power (mW)	Cumulative 39Ar	40Ar/39Ar meas.	+/-	37Ar/39Ar meas.	+/-	36Ar/39Ar meas.	+/-	% Atm. 40Ar	+/-	Ca/K	+/-	Cl/K	+/-	40*/39K	+/-	Age (Ma)	+/- (Ma)
400	0.1568	46.2854	0.1709	0.0008	0.0004	0.0036	0.0002	2.2834	0.1140	0.0015	0.0008	0.0005	0.0001	45.1995	0.1761	278.18	1
600	0.2379	45.5680	0.3247	0.0007	0.0010	0.0013	0.0005	0.8315	0.3227	0.0014	0.0018	0.0005	0.0001	45.1596	0.3552	277.96	2.03
800	0.2952	47.9415	0.3871	0.0643	0.0018	0.0013	0.0005	0.7782	0.3029	0.1180	0.0032	0.0007	0.0001	47.5411	0.4117	291.49	2.33
1000	0.3366	48.6637	0.2870	0.2293	0.0034	0.0005	0.0007	0.2872	0.4130	0.4208	0.0063	0.0017	0.0002	48.5022	0.3500	296.92	1.98
1300	0.3745	51.0297	0.3063	0.0067	0.0023	0.0049	0.0011	2.8287	0.6059	0.0123	0.0042	0.0004	0.0001	49.5576	0.4319	302.87	2.43
1600	0.4045	52.6801	0.3559	0.0077	0.0021	0.0028	0.0010	1.5445	0.5747	0.0141	0.0039	0.0005	0.0002	51.8375	0.4647	315.65	2.6
2000	0.4468	58.1489	0.4190	0.0107	0.0012	0.0033	0.0007	1.6536	0.3538	0.0197	0.0023	0.0008	0.0001	57.1585	0.4634	345.13	2.55
2500	0.4722	59.4629	0.5122	0.1231	0.0026	0.0014	0.0012	0.6644	0.6152	0.2260	0.0048	0.0005	0.0002	59.0435	0.6272	355.46	3.43
3000	0.5309	59.4120	0.3966	0.0725	0.0012	0.0022	0.0005	1.0851	0.2386	0.1331	0.0022	0.0004	0.0001	58.7409	0.4199	353.8	2.3
3500	0.7868	59.1379	0.2488	0.0035	0.0002	0.0022	0.0001	1.1120	0.0674	0.0064	0.0004	0.0005	0.0000	58.4510	0.2498	352.22	1.37
4000	0.8499	63.1699	0.4438	-0.0009	0.0014	0.0021	0.0005	0.9935	0.2419	-0.0017	0.0026	0.0005	0.0001	62.5128	0.4676	374.31	2.53
5000	0.9125	57.3730	0.4934	-0.0010	0.0015	0.0019	0.0004	0.9831	0.1963	-0.0019	0.0028	0.0005	0.0001	56.7795	0.5031	343.04	2.77
6000	0.9936	55.6348	0.4044	0.0011	0.0007	0.0020	0.0005	1.0809	0.2661	0.0020	0.0013	0.0005	0.0001	55.0040	0.4288	333.25	2.37
9000	1.0000	60.0833	0.4766	0.0035	0.0095	-0.0001	0.0041	-0.0458	1.9904	0.0065	0.0174	0.0011	0.0008	60.0812	1.2869	361.12	7.01
Integrated		54.2944	0.0995	0.0226	0.0003	0.0023	0.0001	1.2583	0.0651	0.0414	0.0006	0.0005	0.0000	53.5827	0.1049	325.37	1.05

Sample name: R3 FS#L1 (undeformed).
Location, Mikkelvik, Ringvassøya (70.05195˚N, 19.03317˚E)
Weighted average of J from standards = 3.775e-03 +/- 1.217e-05
Days since irradiation = 64

Laser Power (mW)	Cumulative 39Ar	40Ar/39Ar meas.	+/-	37Ar/39Ar meas.	+/-	36Ar/39Ar meas.	+/-	% Atm. 40Ar	+/-	Ca/K	+/-	Cl/K	+/-	40*/39K	+/-	Age (Ma)	+/- (Ma)
400	0.0016	404.5628	14.8881	0.2915	0.0956	0.1866	0.0316	13.6269	2.2521	0.5349	0.1755	0.0075	0.0056	#####	15.7880	1517.3	46.33
600	0.0254	77.6362	0.5214	0.0300	0.0088	0.0113	0.0018	4.2851	0.6775	0.0550	0.0161	0.0011	0.0004	74.2826	0.7289	445.93	3.88
800	0.0757	62.2980	0.3039	0.0213	0.0041	0.0101	0.0025	4.7760	1.2015	0.0392	0.0075	0.0004	0.0002	59.2953	0.8059	364.41	4.48
1000	0.1332	63.3595	0.3917	0.0238	0.0036	0.0038	0.0009	1.7509	0.3965	0.0436	0.0067	0.0008	0.0002	62.2220	0.4627	380.62	2.55
1300	0.1980	63.1622	0.3769	0.0204	0.0024	0.0029	0.0007	1.3524	0.3149	0.0375	0.0043	0.0009	0.0002	62.2796	0.4238	380.94	2.34
1600	0.2660	60.8711	0.3990	0.0283	0.0028	0.0028	0.0010	1.3528	0.4652	0.0520	0.0051	0.0005	0.0001	60.0195	0.4870	368.44	2.7
1900	0.3319	62.3264	0.4661	0.0831	0.0035	0.0028	0.0009	1.3243	0.4039	0.1525	0.0065	0.0005	0.0001	61.4754	0.5264	376.5	2.91
2200	0.3778	62.8829	0.4132	0.0733	0.0037	0.0007	0.0008	0.3389	0.3774	0.1345	0.0068	0.0006	0.0002	62.6435	0.4759	382.94	2.62
2500	0.4037	63.5695	0.5182	0.0296	0.0098	0.0007	0.0023	0.3018	1.0810	0.0543	0.0179	0.0009	0.0004	63.3493	0.8597	386.83	4.72
3000	0.4310	65.7139	0.4590	0.0330	0.0058	0.0045	0.0014	2.0193	0.6466	0.0606	0.0106	0.0006	0.0003	64.3593	0.6214	392.37	3.4
3500	0.4537	71.8816	0.5486	0.0409	0.0075	0.0042	0.0018	1.7130	0.7350	0.0751	0.0137	0.0008	0.0004	70.6231	0.7569	426.36	4.07
4000	0.4724	81.2569	0.5391	0.0720	0.0095	0.0061	0.0024	2.1988	0.8777	0.1321	0.0175	0.0005	0.0004	79.4452	0.8894	473.18	4.66
4500	0.4828	79.2335	0.9983	0.0656	0.0173	0.0052	0.0035	1.9337	1.3056	0.1203	0.0318	0.0011	0.0008	77.6759	1.4246	463.89	7.5
5000	0.4945	86.6222	0.6531	0.0640	0.0178	0.0087	0.0055	2.9442	1.8669	0.1174	0.0326	0.0011	0.0007	84.0468	1.7378	497.12	8.98
6000	0.5125	92.6633	0.7018	0.0598	0.0091	0.0106	0.0026	3.3591	0.8183	0.1098	0.0166	0.0009	0.0005	89.5257	1.0213	525.22	5.2
9000	0.5364	98.1034	0.6504	0.0393	0.0076	0.0061	0.0019	1.8461	0.5817	0.0722	0.0140	0.0011	0.0005	96.2658	0.8594	559.2	4.29
9001	1.0000	73.4344	0.2904	0.0060	0.0006	0.0027	0.0001	1.0790	0.0581	0.0110	0.0010	0.0008	0.0001	72.6129	0.2908	437.03	1.55
Integrated		70.9856	0.1489	0.0259	0.0008	0.0040	0.0002	1.6502	0.0989	0.0475	0.0015	0.0008	0.0000	69.7863	0.1628	421.86	1.5

Late Permian - Early Triassic Northern Norway Faulting

Sample name: S10/40 FS#L1 (undeformed)
Location: Vannareidet, Vannøya (70.21555˚N, 19.69545˚E)
Weighted average of J from standards = 3.775e-03 +/- 1.217e-05
Days since irradiation = 76

Laser Power (mW)	Cumulative 39Ar	40Ar/39Ar meas.	+/-	37Ar/39Ar meas.	+/-	36Ar/39Ar meas.	+/-	% Atm. 40Ar	+/-	Ca/K	+/-	Cl/K	+/-	40*/39K	+/-	Age (Ma)	+/- (Ma)
400	0.1726	94.4024	0.5787	-0.0027	0.0007	0.0080	0.0003	2.4998	0.0810	-0.0049	0.0012	0.0017	0.0000	92.0134	0.5752	537.84	2.91
600	0.2851	57.2331	0.3300	-0.0034	0.0012	0.0016	0.0003	0.8146	0.1518	-0.0062	0.0022	0.0004	0.0001	56.7373	0.3398	350.12	1.91
800	0.3842	60.7795	0.3371	-0.0026	0.0014	0.0016	0.0004	0.7745	0.1766	-0.0047	0.0025	0.0005	0.0001	60.2792	0.3525	369.88	1.96
1000	0.4216	60.5351	0.7852	0.0007	0.0033	0.0016	0.0010	0.7636	0.4793	0.0013	0.0060	0.0006	0.0002	60.0434	0.8337	368.57	4.63
1300	0.4685	64.7818	0.6437	-0.0096	0.0026	0.0018	0.0007	0.8215	0.3355	-0.0176	0.0047	0.0008	0.0001	64.2197	0.6771	391.6	3.71
1600	0.5142	73.5091	0.7106	-0.0073	0.0033	0.0028	0.0007	1.1273	0.2623	-0.0134	0.0061	0.0007	0.0001	72.6507	0.7326	437.23	3.91
1900	0.5573	73.1119	0.8458	-0.0091	0.0026	0.0017	0.0010	0.7035	0.3823	-0.0167	0.0047	0.0006	0.0002	72.5676	0.8875	436.79	4.74
2200	0.6125	90.1288	0.4356	-0.0053	0.0022	0.0033	0.0007	1.0772	0.2273	-0.0097	0.0040	0.0015	0.0001	89.1282	0.4799	523.2	2.44
2500	0.6699	99.6254	0.5771	-0.0058	0.0019	0.0052	0.0005	1.5484	0.1584	-0.0107	0.0036	0.0017	0.0001	98.0532	0.5936	568.11	2.95
3000	0.6849	94.3463	0.8121	-0.0093	0.0115	0.0046	0.0020	1.4381	0.6272	-0.0170	0.0211	0.0016	0.0004	92.9596	1.0009	542.61	5.04
3500	0.7305	99.2618	0.8074	-0.0042	0.0025	0.0048	0.0007	1.4280	0.2079	-0.0077	0.0046	0.0024	0.0001	97.8148	0.8248	566.92	4.1
4000	0.8111	115.8306	0.6653	-0.0062	0.0016	0.0050	0.0005	1.2644	0.1250	-0.0113	0.0030	0.0026	0.0001	114.3362	0.6765	647.26	3.22
4500	0.8668	116.5661	0.7208	-0.0077	0.0025	0.0084	0.0006	2.1255	0.1466	-0.0141	0.0046	0.0022	0.0001	114.0588	0.7319	645.94	3.48
5000	0.8790	100.0161	1.1946	-0.0181	0.0100	-0.0002	0.0026	-0.0479	0.7535	-0.0333	0.0183	0.0014	0.0004	100.0330	1.4127	577.92	6.98
6000	0.8791	65.4931	8.4316	-0.1683	0.5626	-0.2590	0.1654	-116.9021	73.2709	-0.3088	1.0321	-0.0148	0.0263	141.9745	51.1440	774.13	226.7
9000	0.9278	115.8098	0.6451	-0.0048	0.0025	0.0085	0.0008	2.1682	0.2102	-0.0088	0.0045	0.0023	0.0001	113.2693	0.6830	642.18	3.26
9001	1.0000	125.6387	0.6803	-0.0081	0.0016	0.0048	0.0004	1.1211	0.0956	-0.0149	0.0029	0.0024	0.0001	124.2000	0.6872	693.57	3.19
Integrated		88.9660	0.1682	-0.0052	0.0005	0.0044	0.0001	1.4618	0.0479	-0.0095	0.0010	0.0015	0.0000	87.6359	0.1722	515.58	1.69

DR item 3: Individual $^{40}Ar/^{39}Ar$ age spectra, and Cl/K ratios.

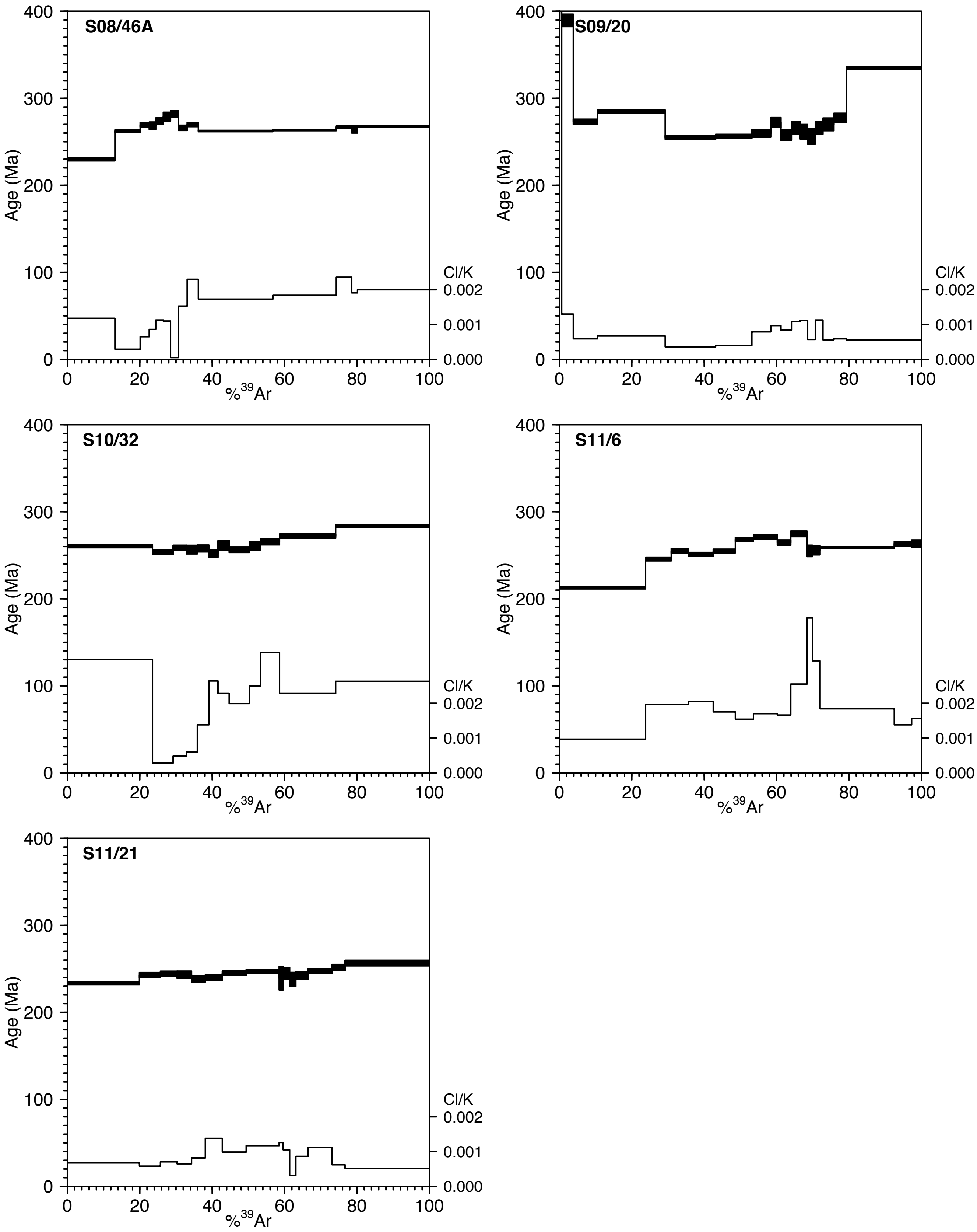
S08/46A
S09/20
S10/32
S11/6
S11/21
Age (Ma)
Cl/K
% ^{39}Ar
0
100
200
300
400
0.000
0.001
0.002
0
20
40
60
80
100

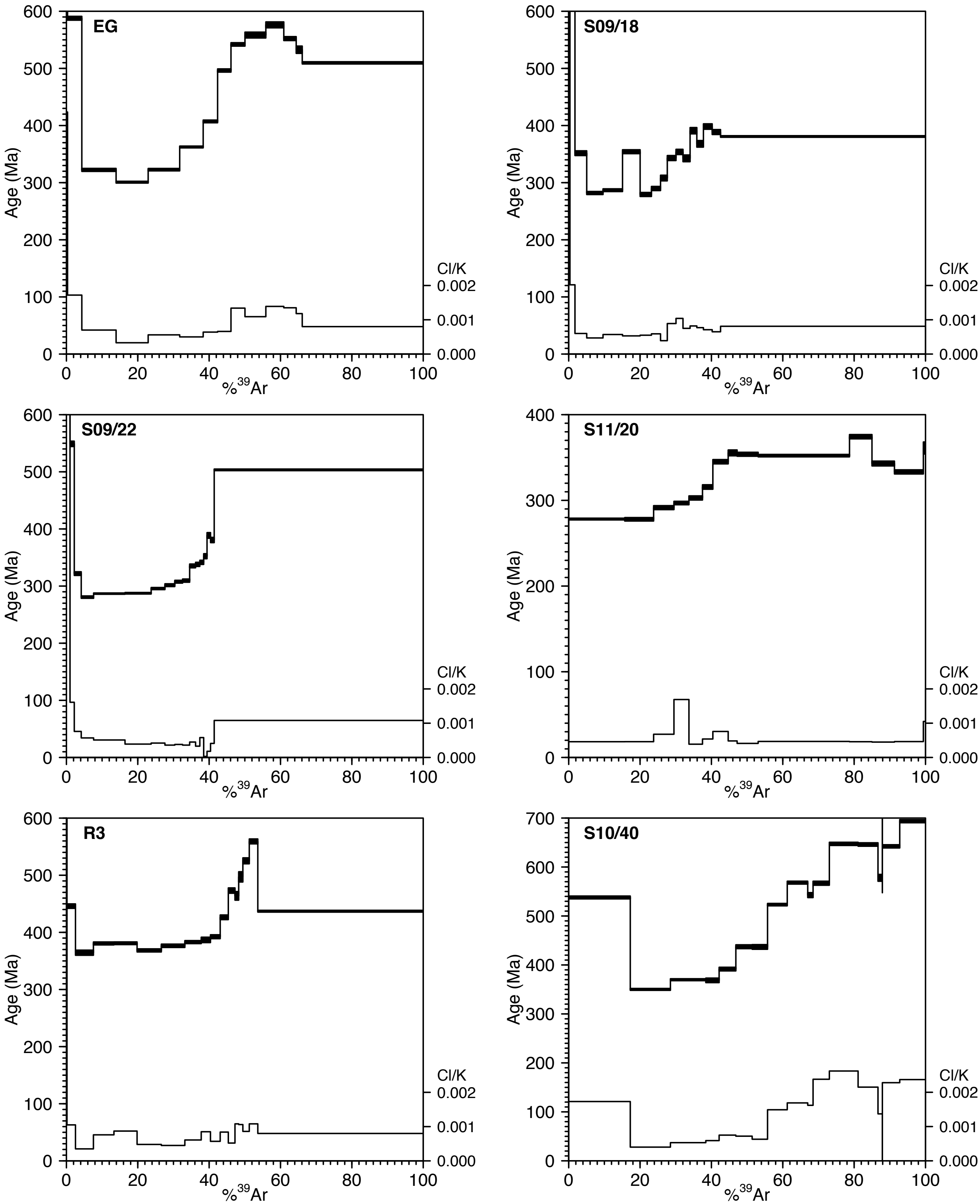
EG
S09/18
S09/22
S11/20
R3
S10/40
Age (Ma)
%39Ar
Cl/K
0.000
0.001
0.002
0
20
40
60
80
100
200
300
400
500
600
700